An adaptive control dynamic-grids generation method for numerical simulation of moving and deforming boundary flow field

***Zeyu GUO[1], † Zuogang CHEN [1,2]**

1 State Key Laboratory of Ocean Engineering, Shanghai Jiao Tong University, Shanghai 200240, China;
2 Collaborative Innovation Center for Advanced Ship and Deep-Sea Exploration(CISSE), Shanghai 200240, China

*Presenting author: sjguozeyu@sjtu.edu.cn
†Corresponding author: zgchen@sjtu.edu.cn

Abstract

A novel adaptive control dynamic-grids generation method based on two-dimensional body fitted grids is developed, which offers a solution to the application of high-precision structured grids in the complicated moving and deforming boundary flow fields. There have been some dynamic-grids methods proposed by researchers. In these methods, advantages of structured grids in the accuracy and rate of generation, and the applicability of turbulence models, have not been made full use of. The adaptive control method manages to generate updated high-precision body fitted structured grids in each time step according to the movement and deformation of flow field boundaries. Researches of flow fields with moving and deforming boundaries are supposed to benefit from this new dynamic-grids method.

Keywords: dynamic-grids; grid generation; body fitted structured grids; deforming boundary flow field; fish-like undulation

Introduction

In the field of simulation and quantification of biological locomotion in fluids, a series of challenges are presented for the development of suitable numerical methods in front of researchers. The movement and deformation of the boundary in an unsteady flow field remains a challenge for numerous CFD researches. The dynamic-grids technology is a commonly used method to tackle with such situation. Then more dynamic-grids methods are proposed and developed by researchers.

The dynamic-grids methods are generally coupled with unstructured triangular grids owing to its brilliant solution to the complex geometric configurations. Cavallon et al. [1] developed an edge-based unstructured flow solver for flow fields with moving and/or deforming boundaries. In the work of Batina [2], an improved algorithms for the solution of the time-dependent Euler equations are presented for unsteady aerodynamic analysis involving unstructured dynamic meshes. Blom [3] presents an investigation on the spring analogy, which serves for deformation in a moving boundary problem. Many researchers have used and improved the spring analogy coupled with unstructured grids in a variety of flow fields. Bottasso et al. [4] complement a network of edge springs with an additional set of linear springs that oppose element collapsing to achieve better robustness. Pérez et al. [5] applied the 2D dynamic mesh based on spring-smoothing dynamic mesh model for deposit shape prediction in boiler banks. However, it is still unable to handle the large deformation using only spring-smoothing method for dynamic-grids. Therefor this method is often coupled with globe or regional remeshing methods.

But the inherent defect of unstructured triangular grids is inextricable. The structured grid has more advantages compared with the unstructured grid in the computer memory saving and the computational efficiency. To employ the structured grids on the dynamic-grids methods, the first requirement is to generate the body-fitted grids for different boundaries. In 1999, the generation of various forms of grids has been systematically introduced [6]. It is a challenge for researchers to maintain the grids quality and orthogonality during the movement and deformation of boundaries. The commercial CFD software, FLUENT, is adopted a dynamic-grids method for structured grids, which is called diffusion-smoothing method. But this method is still of strong limitation. At present, few researchers stimulate the flow fields with moving and deforming boundaries with structured grids, which is a treasure trove for CFD.

With the development of CFD technology, many other methods are introduced into the problem. The wake structure of a single swimmer is simulated by Mattia et al. [7] using a vortex particle method coupled with a penalization technique. Yigang Xu and Decheng Wan [8] approach the problem with multi-block and overset grid method.

We present a novel adaptive control dynamic-grids generation method based on two-dimensional body fitted grids in the paper. The method, which is named as adaptive control dynamic-grids method, aims to solve the application of high-precision structured grids in the complicated flow field of moving and deforming boundaries. It can control the accuracy of structured grids of the entire flow field readily, especially in the near-wall and wake region. The computational expense is less than most present dynamic-grids methods.

Methodology

Structured body fitted grids generation method

The kernel of body fitted structured grids generation is to build up the mapping relation between the computational domain and the physical domain. Many pioneering researchers have proposed various schemes such as the TTM [9] method based on solving a set of elliptic partial differential equations. However, considering that the grids of entire flow field should update in each time steps or certain time steps when using dynamic-grids method, the computational speed and burden are an important factor. As a result, we construct the new method by the algebraic method to achieve the high generating speed. The quality of body fitted grids can be of enough precise. To mapping the physical domain into the computational domain, the Eq. (1) needs to be figured out.

$$
\begin{aligned}
x &= x(\xi,\eta) \quad \xi = \xi(x,y) \\
y &= y(\xi,\eta) ,\; \eta = \eta(x,y)
\end{aligned}
\tag{1}
$$

where Domain ***xy*** refers to the physical domain and Domain ***ξη*** refers to the computational domain. In the application of CFD, the boundary condition is the input parameter, which means that the one-to-one correspondence can be formed between physical domain boundaries and computational domain boundaries. The relation is presented as Eq. (2):

$$
\begin{aligned}
&(x_i, y_{\min}) \Leftrightarrow (\xi_{i,0}, \eta_{i,0}) \qquad (i = 0,1,\ldots,M_x) \\
&(x_i, y_{\max}) \Leftrightarrow (\xi_{i,M_y}, \eta_{i,M_y}) \qquad (i = 0,1,\ldots,M_x) \\
&(x_{\min}, y_j) \Leftrightarrow (\xi_{0,j}, \eta_{0,j}) \qquad (i = 0,1,\ldots,M_y) \\
&(x_{\max}, y_j) \Leftrightarrow (\xi_{M_x,j}, \eta_{M_x,j}) \qquad (i = 0,1,\ldots,M_y)
\end{aligned}
\tag{2}
$$

where M_x and M_y are the number of nodes in x and y dimension separately. In order to implement the coordinate conversion between two different coordinate systems, the Jacobian matrix is introduced. The Jacobian matrix can be deduced as

$$
J = \begin{vmatrix} \xi_x & \xi_y \\ \eta_x & \eta_y \end{vmatrix} = \xi_x\eta_y \text{-} \eta_x\xi_y = \begin{vmatrix} x_\xi & x_\eta \\ y_\xi & y_\eta \end{vmatrix}^{-1}
\tag{3}
$$

where J is the Jacobian matrix. Subscripts represent partial differentiations with respect to the referred variables. It should be noted that these partial differentiations are actually discrete form because the grids nodes are discrete. The computational process is illustrated as Fig. 1 below.

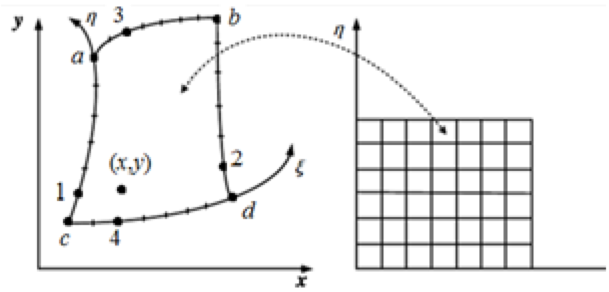

$$
\begin{aligned}
\xi_x &= \frac{1}{x_2 - x_1}, \eta_x = \frac{(y_1 - y_c)/(y_a - y_c) - (y_2 - y_d)/(y_b - y_d)}{(x_2 - x_1)} \\
\eta_y &= \frac{1}{y_3 - y_4}, \xi_y = \frac{(x_3 - x_a)/(x_b - x_a) - (x_4 - x_c)/(x_d - x_c)}{(y_3 - y_4)}
\end{aligned}
\tag{4}
$$

Figure 1 Algebraic interpolation principle

In Eq. (4), subscripts of ξ and η represent the partial differentiations while the subscripts of x and y are the indications of different points as the figure illustrated. The robustness of the computational process is important to deal with various flow field boundaries. There are divisions performed to obtain J. Therefore an extra procedure is applied to complete the coordinate conversion if the denominators happen to be 0 or close to 0.

A subroutine is programmed into the computational process. When the absolute value of the denominator is less than 10^{-6}, the coordinate system is rotated by the subroutine. By rotation of the coordinate of a particular angle, the value of each node is converted and the difference is enlarged to avoid morbid matrix. After the coordinate values of all nodes in the new coordinate system are achieved, let the coordinate just rotate backward by the same angle. By completing the steps above, the grids generation is of generality for different flow field.

Adaptive control dynamic-grids method

Commercial software (FLUENT) has several built-in methods, which can help users to solve dynamic-grids problem readily. But yet, these methods are not able to satisfy researches of various flow fields universally.

The adaptive control dynamic-grids method is coupled with the User Define Function (UDF) based on FLUENT. The UDF is written by the users themselves in C code. Actually, users are able to interfere in any steps of the entire process and redefine them by UDF. However, most of the dynamic-grids applications based on UDF are confined to the moving rigid boundary or unstructured grids. We present the new dynamic-grids method based on structured grids to solve the moving and deforming boundary flow field problem, which is a breakthrough for structured dynamic-grids.

The key part of dynamic-grids is how to control the movement of boundaries and the update of grids. For instance, when a flexible object is locomote in a flow, the movement and deformation occurs simultaneously, which is a challenge for the quality of grids. The software has provided several functional interfaces to settle the dynamic boundaries, while there is hardly any one of them that has been used to control the nodes system of the entire flow field. Fig. 2 presents the process diagram of the adaptive control method.

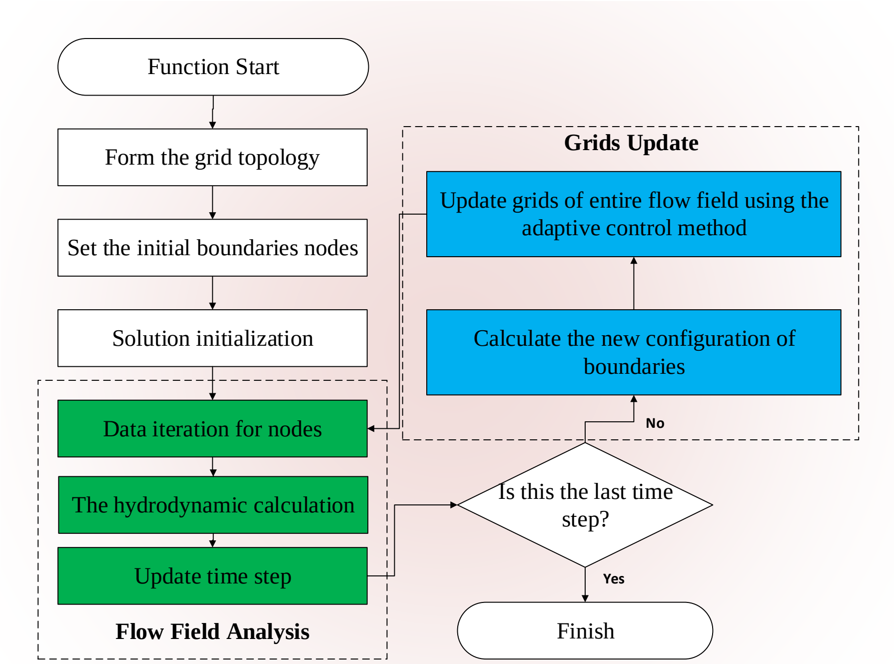

Figure 2: the process diagram of the adaptive control dynamic-grids method

In the Grids Update step, some functions and function functional interfaces are adopted by UDF. The adaptive control method manages to employ the DEFINE_GRID_MOTION functional interface in the entire flow field instead of only boundaries. Firstly, function NODE_X and function NODE_Y traverse all nodes to get their coordinate information. And then, the location and configuration of boundaries are defined according to motion equations. Afterward, the new grids of present time step can be generated by the algebraic interpolation mentioned above.

During the update process, the sequence of nodes is rigid when functions traverse and coordinates update, which needs extra attention. The match-up of the original nodes and update nodes is important for the date iteration. To arrange the node sequence properly, we number all the nodes and the sequence number is used to iterate back the update coordinates and other discrete flow field data.

Due to the complete control of grid nodes, the quality of grids does not depend on smooth models of FLUENT. The quality of both globe and regional grids can be assured by adjusting the UDF. In general, the adaptive control dynamic-grids method updates grid nodes in each time step rapidly and control the spacing of boundaries to assure the grid quality and orthogonality.

Application and Validation

In hydrodynamic researches concerning fish swimming, the hydrodynamic characters of flexible boundaries remain a hot spot. The high propulsive efficiency and energy saving locomotion style of fish undulation are attractive for scientists to study and simulate. Research of flexible body locomotion is subject to the difficulties of dealing with moving and deforming boundaries. Methods provided by most CFD softwares are still not able to settle the problem perfectly. To validate the advantages of the adaptive dynamic-grids method, we compared it with several other methods in a fish-like undulation flow field.

The moving and deforming boundary problem of fish-like undulation

The simulated body undulates actively in unbounded oncoming flow. Related variables are normalized by the body length L and oncoming velocity U, as well as the time is normalized by L/U. The movement of the undulating body in y direction is given as

$$y(x,t) = ax^n \sin[2\pi b(x - Sp \cdot t)] \tag{5}$$

where a is amplitude, n=1.1, $2\pi b$ is wave number, Sp is phase velocity, t is time, where x and y are the stream-wise and the lateral coordinates whose origin locates at the leading edge of the body. $0 \leqq x \leqq Xend(t)$ where $Xend(t)$ is x-coordinate of the trailing edge calculated as

$$\int_0^{Xend(t)} \sqrt{1+\left(\frac{\partial y}{\partial x}\right)^2}\, dx = 1.0 \tag{6}$$

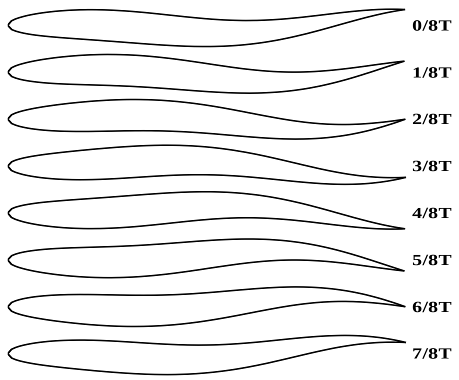

Figure 3: Configurations of an undulating NACA0010 during one period (a=0.051, b=1.0)

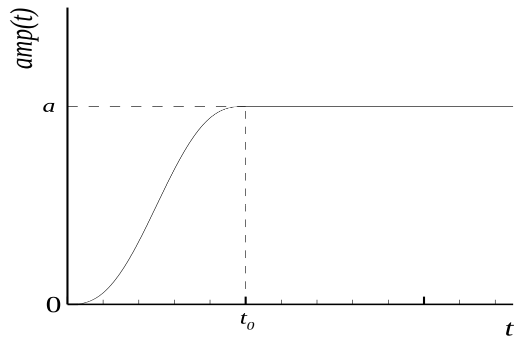

Figure 4: Employed acceleration modes for undulating amplitude

Equation (2.2) keeps the body length constant during the undulation. The obtained smooth deforming surface of NACA0010 can be seen in Figure 3.

In the present study, in the flow field acceleration stage, which is within the non-dimensional time, the undulating amplitude increase from zero to a final constant. As shown in Fig.4, when $t \geq t_0$, it keeps constant. The acceleration model satisfies Eq. (7):

$$amp = \begin{cases} at^3(6t^2 - 15t + 10) & 0 \leq t \leq 1 \\ a & t > 1 \end{cases} \tag{7}$$

It is noted that the boundary of the fish body is flexible. When the fish is swimming, the movement and deformation of the boundary both occur, which lead to the enormous problems of dynamic-grids.

Application of present dynamic-grids methods

In the simulation of fish undulation flow field, on the one hand, the movement and deformation of boundaries are of significance. On the other hand, a finer grid scheme in the boundary layer region should be maintained consistently. As different turbulence models have different requirements for the grids quality in the boundary layer region, the initial spacing of boundary grids must be carefully maintained to meet various requirements during the dynamic computation

The spring-based smoothing method regards the edges between any two grid nodes as a network of interconnected springs. When the grids deteriorated because of the boundary displacement, a remeshing method will be enabled to update the new grids to avoid convergence problems.

In Fig. 5, different remeshing parameters are chose for the triangular grids. The Maximum Length Scale (MLS) parameters, which specifies the upper limit of cell size above which the cells are marked for remeshing, are 0.01 for Fig. 5(a) and 0.001 for Fig. 5(b). When the MLS is 0.01 which is relatively a large number, the alteration of the globe grids is slight. While if MLS becomes 0.001, which is relatively a small number, clusters of dense grids appear stochastically. To obtain acceptable grids, many researchers have made lots of improvements for the choices of relevant parameters based on their particular projects. But the disadvantages of unstructured triangular grids on the study of the boundary layer are inevitable.

The diffusion-smoothing method is proposed based on structured grids. The grids motion is governed by a diffusion equation, which is a Laplace equation. The equation describes how the prescribed boundary motion diffuses into the interior grids. Fig. 6(*a*) and Fig. (*b*) show the grids at t=1 and t=6 separately. When the fish just finished the acceleration at t=1, the orthogonality of grids in the near-wall region is no longer as good as the initial grids. When computation proceed to t=6, the skewness of structured quadrilateral grid in some regions, especially in the intense motion region, is so deteriorated that the convergence problem may happen. Compared with spring-smoothing method, the diffusion-smoothing method is computationally more expensive but is able to achieve better grid quality.

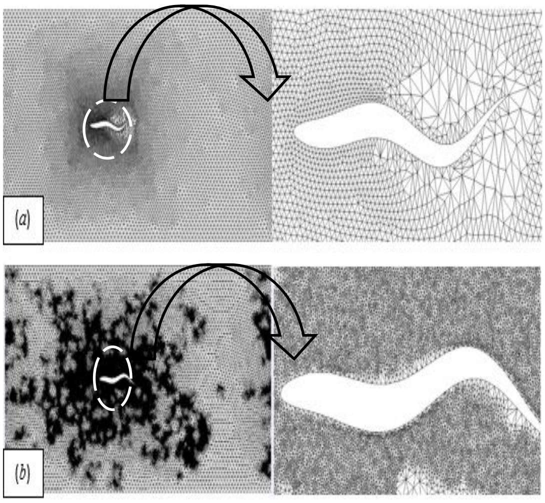

Figure 5: Grids based on spring smoothing and remeshing method at different Maximum Length Scale

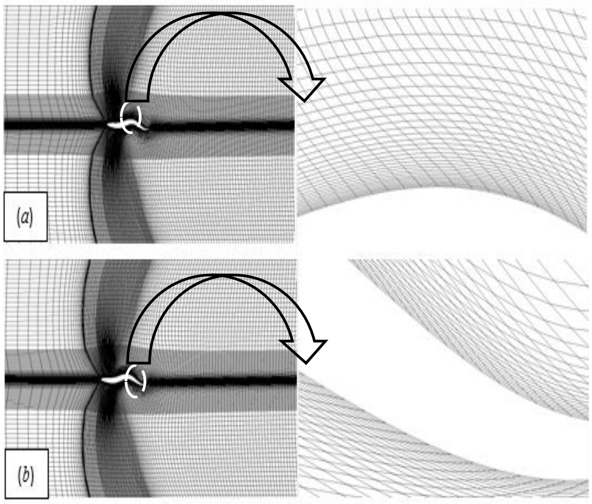

Figure 6: Domain grid and grid at boundary layer based on diffusion-smoothing method at *t*=1 (*a*) and *t*=6 (*b*)

In the overset grid method, the background grid and the embedded grid are generated independently. When the fish swims, only the embedded grid need to move and deform without having to remesh the background grid. The connection between background and the embedded grid is the interfaces, which interpolate cell data in overlapping regions. To avoid the interpolation errors, the embedded region must overlap sufficiently, which is expensive computationally.

Application of Adaptive control dynamic-grids method

The initial grid topology of the adaptive control dynamic-grids method is similar with the diffusion-smoothing method besides the enhancement of boundary and wake grids. The computational domain is $-3.0 \leqq x \leqq 5.0$, $-2.0 \leqq y \leqq 2.0$, where the coordinates are normalized by fish length L. The grid consists of [140×195] points in x, y directions where minimum normal spacing is 2×10^{-5} to meet the requirement of SST turbulence model. The obtained grids movement and deformation can be seen in Fig. 7.

During one complete period of a fish undulation (Fig. 7), the density of grid nodes maintains consistently. Although the motion of boundary is intense, the orthogonality of grid in the near-wall region is well preserved. Considering the wake flow of the fish undulation, grids in the wake region are diffused gradually. Moreover, the edge curvature of grid cells are correlated with the camber line of the fish body. From the generation method aforementioned, it can be noticed that the update grids in new time step are independent of the grids in last time step, which means that the quality of grids will not deteriorate time-dependently. When the movement and deformation of boundaries are cyclical, the motion of grids can be accordingly cyclical by using this new method, which ensure the quality of grids and the accuracy of computation.

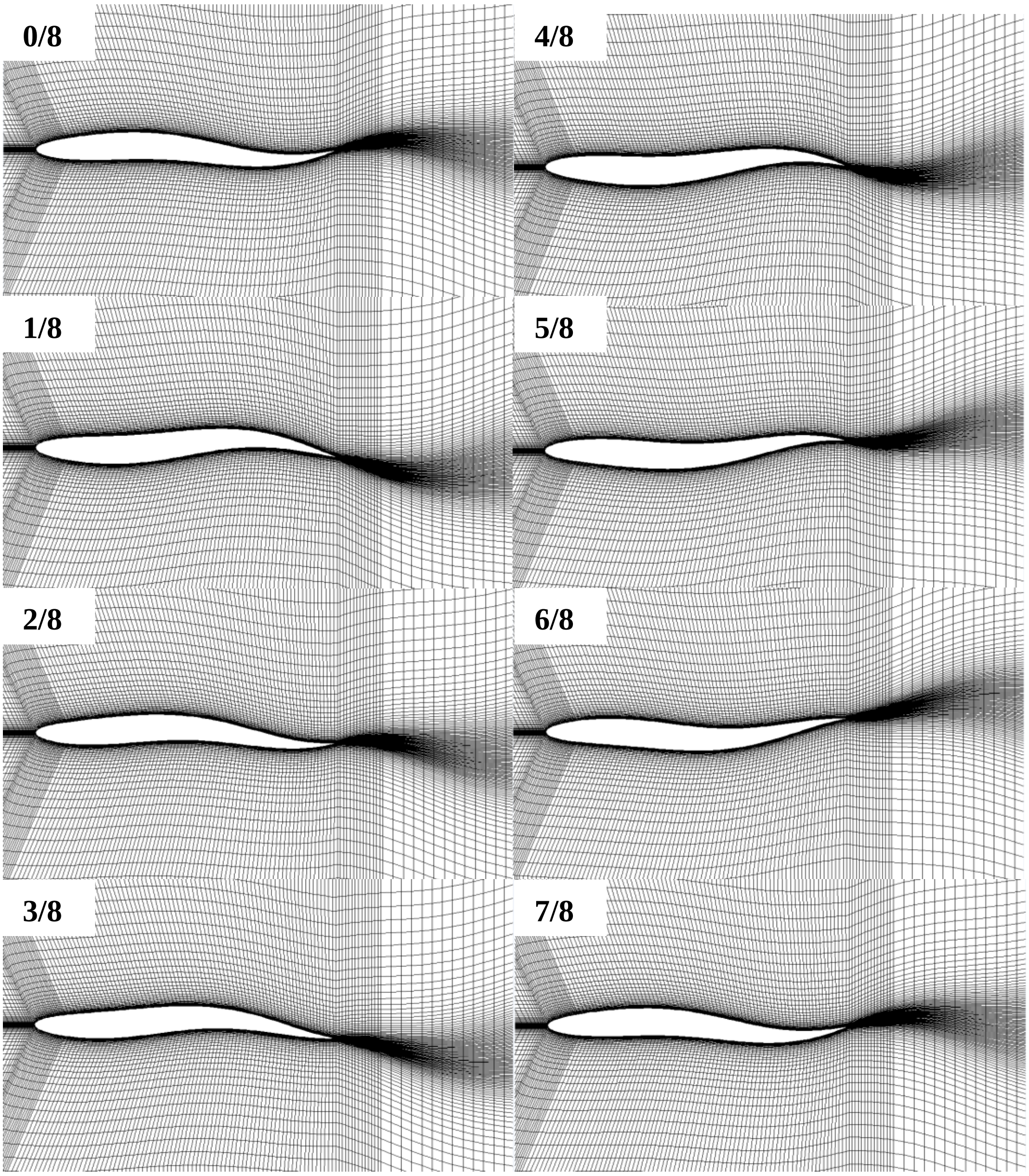

Figure 7: The dynamic movement and deformation of structured grids based on the adaptive control method during one period (*a*=0.051, *b*=1.0)

Validation on hydrodynamic force coefficients and

The total force acting on the body varies during the undulating motion. Therefore, in the present study, self-propulsion is defined as the condition when the time-averaged total force becomes zero. The hydrodynamic force coefficients are defined as follows[10]:

$$C_{Fx} = \frac{F_{xf}}{\frac{1}{2}\rho U_0{}^2 S}, C_{Px} = \frac{F_{xp}}{\frac{1}{2}\rho U_0{}^2 S} \tag{8}$$

$$\overline{C}_{Fx} = \frac{\int_0^T F_{xf}\,\mathrm{dt} \Big/ T}{\frac{1}{2}\rho U_0{}^2 S}, \overline{C}_{Px} = \frac{\int_0^T F_{xf}\,\mathrm{dt} \Big/ T}{\frac{1}{2}\rho U_0{}^2 S}, \overline{C}_{Tx} = \overline{C}_{Fx} + \overline{C}_{Px} \tag{9}$$

where F_{xf} is x-component of frictional force exerted on the body, F_{xp} is x-component of pressure exerted on the body, T is the period of the undulation, ρ is the density of the fluid, U_0 is the oncoming velocity, S is the area of the body. The negative symbol of pressure component F_{xp} (against to x-axis) represents thrust and the positive symbol of frictional force component F_{xf} (same to x-axis) represents resistance. When the self-propulsion condition is achieved, the time-averaged total force exerted on the body becomes zero. The hydrodynamic force coefficients computed by these methods mentioned above are compared. C_{Fx}, C_{Px} and C_{Tx} are the primary focus.

Fig. 8 presents the simulated time history of hydrodynamic force coefficient C_{Fx} of overset grid method. The computed curves of C_{Fx} oscillate by time with large noise as shown in Fig. 8. The noise comes from the interpolation errors resulted from the data exchange. The noise can be decreased by densifying background grids, which causes the computational expense increased significantly. Nevertheless, encryption can only attenuate the noise, but it is unable to remove the noise completely.

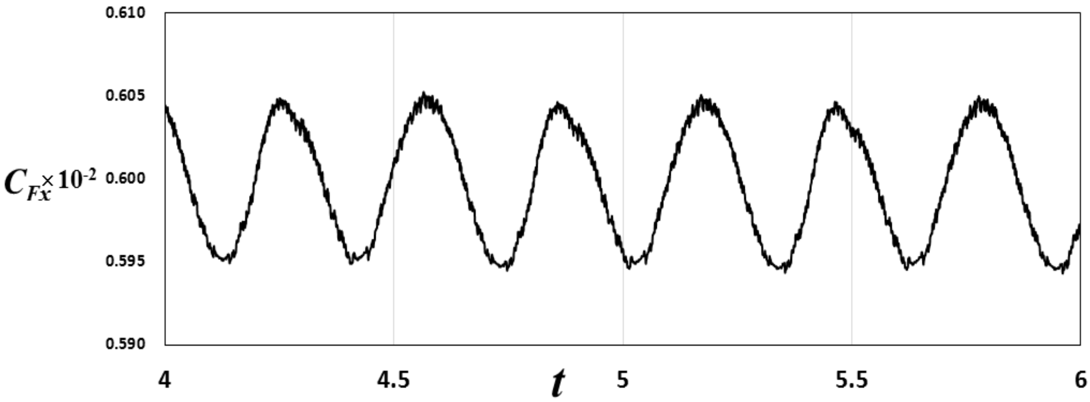

Figure 8: Simulated time history of hydrodynamic force coefficients at (Re=10^7, a=0.051, b=1.5, Sp=1.17) based on overset grids method

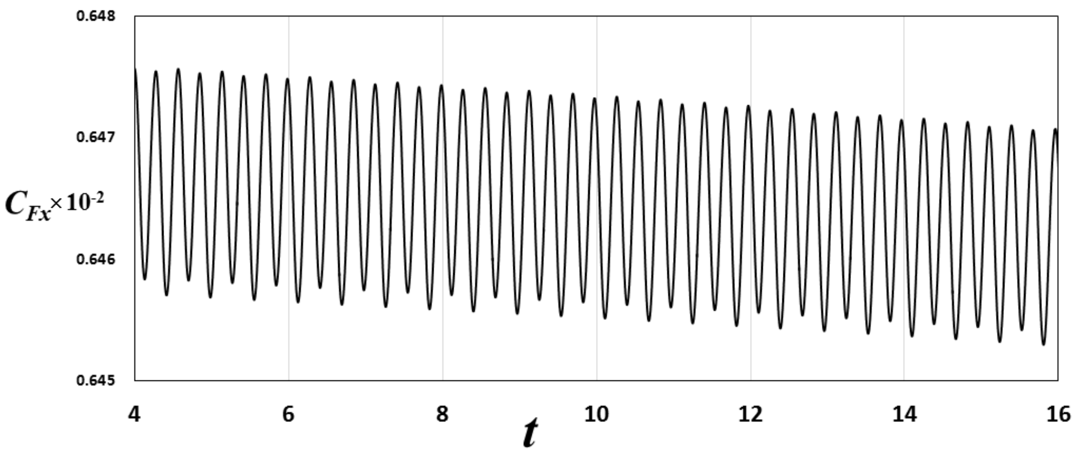

Figure 9: Simulated time history of hydrodynamic force coefficients at (Re=10^7, a=0.051, b=1.5, Sp=1.17) based on diffusion-smoothing method

Fig. 9 is the computed results of diffusion-smoothing method. The time-averaged value of C_{Fx} gradually decrease with the periodical locomotion of fish, which means that the result is unauthentic. If finer grids with smaller height value of the first boundary layer grids are adopted to meet the requirement of advanced turbulence models, the deterioration of grids quality will lead to computational divergence.

The results of the adaptive control method are presented in Fig.10. Simulated time history of indicates that the self-propulsion condition is achieved. All the hydrodynamic force coefficients are continuous and smooth, and undulate periodically. The results will not be deteriorative or even divergent as computation goes on.

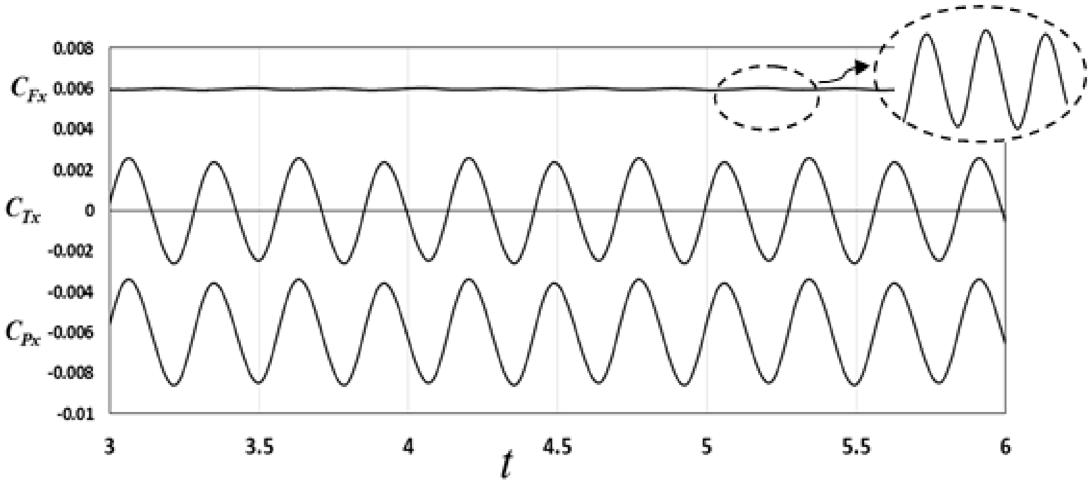

Figure 10: Simulated time history of hydrodynamic force coefficients at （*Re*=10^7，*a*=0.051，*b*=1.5，*Sp*=1.17）based on adaptive control method

The structure and characteristics of the flow field are also part and parcel of the computation. The globe and regional velocity contours based on the adaptive control method and the spring smoothing method are compared in Fig. 11. The globe velocity contours are similar, while in the wake region, the obvious differences can be noticed. The adaptive control method better simulates the process of shedding vortices, which is expected to be smooth without noise according to the previous works.

If more detailed observation is taken on the boundary layer, significant errors will be noticed in the boundary layer calculated by the spring-smoothing method. Because of the limitation of unstructured grids on the simulation of the flow field in near-wall region, the accurate flow field can hardly be achieved. The shape of grid cells has evident influences on the contours, which lead to the uncertainty of computation.

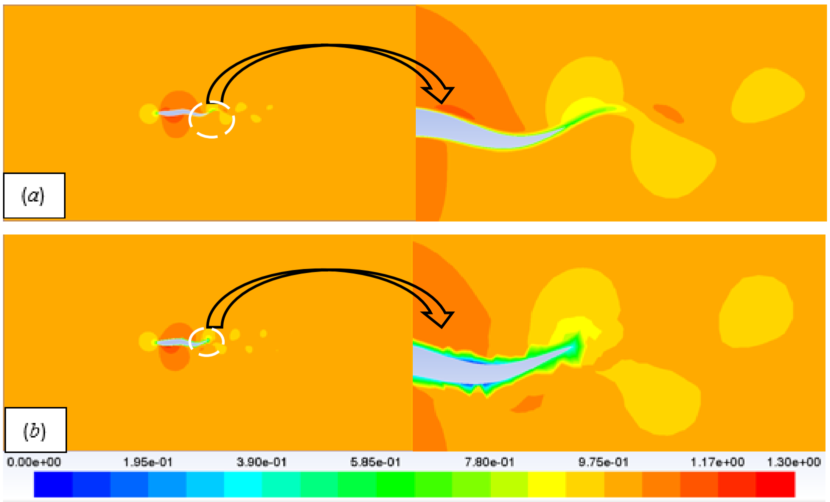

Figure 11: Velocity contours based on adaptive control method (*a*) and spring-smoothing method (*b*) method

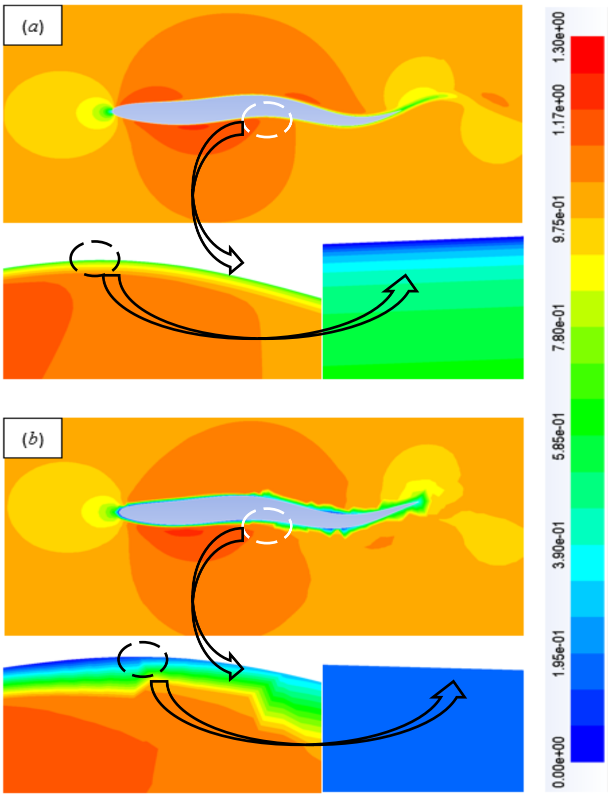

Figure 12: Boundary layer based on adaptive control method (*a*) and spring-smoothing method

The velocity contours illustrate that a row of low velocity zones appear in the wake of fish undulating. With the help of accuracy computational results based on the adaptive control method, the complete process of the shedding vortices can be simulated and researched. Fig. 13 illustrates the morphology of the wake and the flow adjacent to the fish body. The results are also compared with previous experimental and numerical research. The vorticity distributions are correspondent to the experimental flow field of a swimming eel visualized by

PIV[11]. The wake structure resembles a reverse von Karman vortex street. The numerical simulation of Chen [10] and Mattia[7] with different methods came to the similar conclusion.

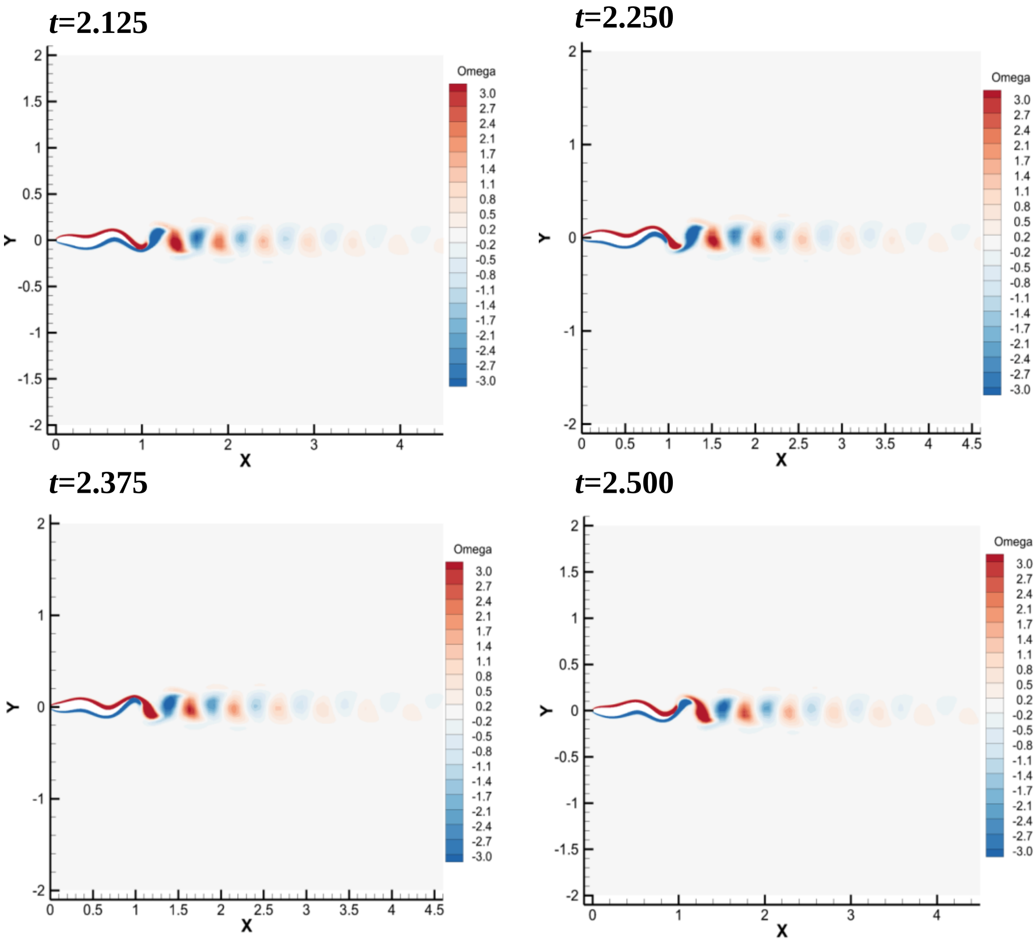

Figure 13: Vorticity contour of the wake flow field by adaptive control dynamic grids method

Concluding Remarks

Numerous dynamic-grids methods have been proposed by previous researchers for the flow fields with moving and deforming boundary. But these methods are not able to solve this problem perfectly. In the paper, the adaptive control dynamic-grids method is compared with several methods by being adopted in a fish-like undulation flow field

The method is based on structured grids, which can achieve higher grid quality in the near-wall region and the wake. The deterioration of grid quality can be avoided with the solution processing. There is no interpolation error, which is inevitable when using overset grid method. Some frequent problems occurred in previous dynamic-grids methods, including grids intersection and quality deterioration, are solved efficiently. Especially in the boundary layer region, the quality of near-wall structured grids can be guaranteed, which is vital to match up with advanced turbulence models. The comparisons have demonstrated advantages of the new methods in grids quality, the computational cost and the simulation accuracy. These advantages make it an efficient alternative dynamic-grids method to assist with related research.

References

[1]. Cavallo, P., Hosangadi, A., Lee, R., Dash, S., Cavallo, P., Hosangadi, A. & Dash, S. (1997). Dynamic unstructured grid methodology with application to aero/propulsive flowfields. In 15th Applied Aerodynamics Conference (p. 2310).

[2]. Batina, J.T., Implicit flux-split Euler schemes for unsteady aerodynamic analysis involving unstructured dynamic meshes. Aiaa Journal, 2012.

[3]. Blom, F.J., Considerations on the spring analogy. International Journal for Numerical Methods in..., 2015.

[4]. Bottasso, C.L., D. Detomi and R. Serra, The ball-vertex method: a new simple spring analogy method for unstructured dynamic meshes. Computer Methods in Applied Mechanics and Engineering, 2005. 194(39-41): p. 4244-4264.

[5]. Pérez, M.G., E. Vakkilainen and T.H. Nen, 2D dynamic mesh model for deposit shape prediction in boiler banks of recovery boilers with different tube spacing arrangements. Fuel, 2015.

[6]. Thompson, J. F., Soni, B. K., & Weatherill, N. P. (Eds.). (1998). Handbook of grid generation. CRC press.

[7]. Gazzola, M., et al., Simulations of single and multiple swimmers with non-divergence free deforming geometries. Journal of Computational Physics, 2011.

[8]. XU, Y. and D. WAN, Numerical simulation of fish swimming with rigid pectoral fins. Journal of Hydrodynamics, Ser. B, 2012. 24(2): p. 263-272.

[9]. Thompson, Joe F., Frank C. Thames, and C. Wayne Mastin. "Automatic numerical generation of body-fitted curvilinear coordinate system for field containing any number of arbitrary two-dimensional bodies." Journal of computational physics 15.3 (1974): 299-319..

[10]. Chen Z, Doi Y. Numerical Study on Propulsion by Undulating Motion in Laminar-Turbulent Flow [C]. 24th Symposium on Naval Hydrodynamics, Fukuoka, Japan, July 8-13, 2002..

[11] Müller U K, Smit J, Stamhuis E J, et al. How the body contributes to the wake in undulatory fish swimming[J]. Journal of Experimental Biology, 2001, 204(16): 2751-2762.